Journal of Theoretical and Computational Chemistry
Vol. 5, No. 2 (2006) 151–161


World Scientific
www.worldscientific.com

# A MONTE CARLO SIMULATION OF MAGNETIC ORDERING IN ISING FERRITES OF FORMULA $5Fe_2O_3.3Y_2O_3$ WITH GARNET STRUCTURE

NICOLAE STANICA*, GIANINA DOBRESCU and LUMINITA PATRON
*Institute of Physical Chemistry*
*Splaiul Independentei 202, Bucharest 77208, Romania*
**nstanica@icf.ro*

SOONG-HYUCK SUH
*Department of Chemical Engineering, Keimyung University*
*Taegu, 704-701, Korea*

FANICA CIMPOESU
*Department of Chemistry, Graduate School of Science*
*Tohoku University, Aramaki, Aoba-ku Sendai 980-8578, Japan*

LUCIAN POSTELNICU
*Department of Chemistry, Boston University, 590 Commonwealth Avenue*
*Boston, Massachusetts 02215*

Received 24 August 2005
Accepted 17 November 2005

The magnetic properties simulation of extended networks containing quantum spins, by original FORTRAN code "MCIsing", is presented. The computer code is based on Ising model and uses Monte Carlo-Metropolis (MCM) algorithm. The results of magnetic Monte Carlo studies on a garnet type lattice, Ising model ferrimagnet, provide insights into the exchange interactions involved in the Ferrites of Formula $5Fe_2O_3.3Y_2O_3$ with Garnet Structure.

*Keywords*: Ferrimagnet; Cubic ferrospinels; garnet type lattice; Ising-Monte Carlo study.

## 1. Introduction

Cubic iron garnets of formula $A_3Fe_5O_{12}$ are a large class of ferrimagnetic oxides which have applications in magneto-optical devices, waveguide optical isolator and magnetic bubble memories.[1] The study of ultrathin metallic magnetic films is an active field where many efforts are being devoted to investigate the dimensionality effects, anisotropy, interfacial properties, giant magnetoresistence and

magneto-optical properties.[2] When magnetic layers become very thin, their properties depart from those of bulk materials due to new low-dimensional magnetic interactions. Although thin magnetic-oxides are less studied, many interesting magnetic interactions are expected to occur in ultrathin magnetic oxides films. We expect that a Monte Carlo Simulation of Magnetic Ordering in Ising Ferrites of formula $Fe_2O_3.3R_2O_3$ with Garnet Structure (where $R^{3+} = Y^{3+}$, $Gd^{3+}$ or a rare-earth ion), must be the next step[3] in testing MCIsing code, by classical theoretical and experimental results on bulk samples. Subsequently, it can be used for low-dimensional samples in order to study the finite size effect in magnetical properties.

The two crystal types, the most intensely investigated ferrimagnets, are known as "spinel" and "garnet", classes of materials with important technical applications; it is now well known that the spinel and garnet structures are favorable to ferrimagnetism.[4]

Following Néel's suggestion,[5] the name ferrimagnetism is used to cover the behavior of materials in which the overall spontaneous magnetization is a resultant of two or more sublattice magnetizations of this kind. Generally, it is the crystal structure of a ferrimagnetic compound that determines the detailed form of the ordering into magnetic sublattices. The general chemical formula for the compounds which may crystallize in the garnet structure is the complex oxides formula, $A_3B_2X_3O_{12}$, where

- A site distorted cubic environment;
- B/X octahedral & tetrahedral sites.

A typical garnet, grossularite,[6,7] with ideal formula $Ca_3Al_2Si_3O_{12}$, belongs to space group $O_h^{10} - Ia3d$ with $Ca^{2+}$ ions in 24c, $Al^{3+}$ ions in 16a, $Si^{4+}$ ions in 24d and $O^{2-}$ ions in 96 h.[4] Structure for Rare Earth Iron Garnets (REIG) e.g. $Ln_3Fe_5O_{12}$ and $Y_3Fe_5O_{12}$ (ytrium iron garnet, YIG) was established, realizing the substitutions[8]

$$Ca^{2+}(24c) + Si^{4+}(24d) \rightarrow R^{3+} + Fe^{3+}, \qquad Al^{3+}(16a) \rightarrow Fe^{3+}$$

As a result, $Fe^{3+}$ is in the octahedral positions 16a, and in the tetrahedral positions 24d, while R, a rare earth or ytrium ion, is in the positions 24c, centre of highly deformed cubes.

The magnetic moments in 24d and 16a positions are antiferromagnetically coupled and oriented along the body diagonal.[9,10] In heavy REIG, at room temperature, the magnetic structure of the iron sublattice is the same as in YIG, the magnetic moment of $RE^{3+}$ is antiparallel to the total magnetic moment of the iron sublattice.[11] There is a useful drawing[4] where only the metal ions in the four front octants are shown. The Full Cubic Elementary Cell (FCEC or unit cell) refers to all the eight octants from that drawing. $Y_3Fe_5O_{12}$ (YIG) is the prototype for the Rare Earth Iron Garnets (REIG); its crystal structure was described in the space group Ia3d[12] and the coordinates of the metal ions (crystal data)

represent the starting point in our MCIsing Fortran Computer Code. The 1D, 2D, or in our case, 3D metal ions sites network is generated by a subroutine of MCIsing Code, using metal ions's coordinates[12,13] from the first FCEC (unit cell).

The first idea of ferrimagnetic structures as interpenetrant magnetized sublattices came from Néel's quantitative interpretation[5] of the magnitudes of low temperature saturation moments for some simple ferrites. For more complex systems involving many sublattices or canted moments the net spontaneous magnetization is not very informative, so other experimental or theoretical methods for detecting magnetic ordering on the sublattices are required.

For canted materials in particular, the application of large enough magnetic field to align $M_s$ against anisotropy can modify[14] the pattern of ordering. Neutron diffraction from a magnetite crystal provided the first direct confirmation of Néel hypothesis of interpenetrant differently oriented magnetic sublattices. Neutron experiments[15] have shown, in fact, that there are several kinds of ferrimagnetic ordering involving canted spins, as well as the straightforward co-linear arrangements of the simple ferrites. Magnetic measurements[14,16–19] of resultant spontaneous magnetizations or magnetic susceptibility[20] for ferrimagnetic samples suppose particular theoretical models[21–24] in order to separate the sublattice magnetizations and show the inadequacies of the molecular-field models.[26]

In principle, the mean field approximation can be applied in the paramagnetic region and in the ordered phase; however, this method leads to a large overestimation of the ordering temperature.[26] The differences between the specific heat obtained by the mean field approaches and the experimental values are closely associated with spontaneous sublattice magnetizations; they are due to the neglect of the energy associated with short-range order.

We demonstrate that besides the neutron-diffraction method, Ising-Monte Carlo simulation based on the Metropolis algorithm could possibly determine Néel (or Curie) temperature $T_N(T_C)$, compensation temperature, variation with temperature of spontaneous sublattice magnetizations, and magnetic susceptibility. This paper presents the results of Monte Carlo simulations of an Ising ferrimagnet on a YIG garnet type lattice. This work presents new advances in the simulation of the magnetic properties of extended network containing quantum spin.[3]

## 2. Methodology

The Ising Spin model was chosen for this study, since it is known to show a transition to the long-range order at a finite, non-zero temperature.[27] Among the variety of approximate methods available in the literature, the Monte Carlo technique (MC), based on the Metropolis algorithm,[28] generates a sampling of states following the Boltzmann distribution that preferentially contains configurations which minimize interaction energy of the system and bring important contributions for

Table 1. Samples sizes used in simulations.

| Nr. of FCEC for Sample | Nr. of Metal Ions for MC Analysis | Nr. of "nn" Metal Ions from Extension for PBC Conditions | Nr. "Surface" Sites / Nr. Bulk Sites |
|---|---|---|---|
| 8 | 512 | 458 | 0.895 |
| 27 | 1728 | 974 | 0.564 |

magnetization at temperature T.[29] All simulations were performed on finite samples, thus systematic errors may be present. To minimize these errors, the edge perturbation and to accelerate convergence towards the infinite lattice limit, periodic boundary conditions (PBC) were adopted.[30] To obtain reliable results, the optimal sizes of the samples were determined by carrying out simulations on a range of different sample sizes. The minimum size that showed a finite-size effect for the studied reduced temperature range, kT/ |Jab|, was only from one Full Cubic Elementary Cell (FCEC). The tested samples sizes are presented in Table 1.

As the CPU time increases significantly with the size of the Monte Carlo analyzed sample, the results of this paper are obtained at the beginning by using 27 FCEC sample, then for better statistics, we use 8 FCEC sample in the same runtime (100 hours for each case). The results from both cases (8 FCEC sample or 27 FCEC sample) are the same, meaning that the same critical temperatures, magnetizations or susceptibilities versus T are obtained. For each site, at least $10^4$ Monte Carlo steps were performed (MCS) and first $5 * 10^3$ were discarded as the initial transient stage.[30] To avoid a freezing of the spin configuration,[30] we have used a low cooling rate according to the following equation:

$$(P_0)_{i+1} = 0.99 * (P_0)_i \tag{1}$$

where $P_0 \equiv \frac{kT}{|J_{ad}|}$, the reduced temperature parameter.

A periodic boundary "garnet lattice" with 512 (8 FCEC) or 1728(27 FCEC) sites was populated with two (or three, for $Gd_3Fe_5O_{12}$ case) spin types, $S^{24(d)}_{Fe^{3+}} = 5/2$, $S^{16(a)}_{Fe^{3+}} = 5/2$ $(\pm 5/2, \pm 3/2, \pm 1/2)$ (or $S^{24(c)}_{Gd^{3+}} = 7/2$ $(\pm 7/2, \pm 5/2, \pm 3/2, \pm 1/2)$ on two or three separate sublattices: tetrahedrally coordinated $Fe^{3+}$ ions in 24(d) sublattice, octahedrally coordinated $Fe^{3+}$ ions in 16(a) sublattice and dodecahedrally coordinated $Y^{3+}$ or $Gd^{3+}$ ions in 24(c) sublattice. Initial spin states were randomly assigned.

The energy of each "a" site was calculated from the Hamiltonian:
For each "a" site:

$$E_i^a = g_i \mu_B H_z S_{zi}^a + D_i^a \left(S_{zi}^a\right)^2 - 2J_{ad} \sum_{n_d} S_{zi}^a S_{zj}^d$$
$$- 2J_{ac} \sum_{n_c} S_{zi}^a S_{zk}^c - 2J_{aa} \sum_{n_a} S_{zi}^a S_{zj}^a \tag{2}$$

for each "d" site:

$$E_i^d = g_i \mu_B H_z S_{zi}^d + D_i^d \left(S_{zi}^d\right)^2 - 2J_{da} \sum_{n_a} S_{zi}^d S_{zj}^a - 2J_{dc} \sum_{n_c} S_{zi}{}^d S_{zi}^c - 2J_{dd} \sum_{n_d} S_{zi}^d S_{zi}^d \tag{3}$$

and for each "c" site :

$$E_i^c = g_i \mu_B H_z S_{zi}^c + D_i^c \left(S_{zi}^c\right)^2 - 2J_{ca} \sum_{n_a} S_{zi}^c S_{zj}^a - 2J_{cd} \sum_{n_d} S_{zi}{}^c S_{zi}^d - 2J_{cc} \sum_{n_c} S_{zi}^c S_{zi}^c \tag{4}$$

where $n_a$, $n_d$ or $n_c$ indicate summation over the nearest neighbours ("nn") from sublattices "*a*", "*d*" or "*c*". $J_{ad}$, $J_{ac}$, $J_{cd}$ are the nearest neighbour exchange constants between the "*a*", "*d*" and "*c*" spin sublattices and $J_{aa}$, $J_{dd}$ or $J_{cc}$ indicate the nearest neighbor exchange constant between the sites within the same sublattice "*a*", "*d*" or "*c*", depending on the sublattice to which "*i*" belongs.

We have considered for the nearest-neighbor exchange parameters:

- $J_{ad}$ and $J_{cd}$ antiferromagnetic interactions;
- $J_{ac}, J_{aa}, J_{dd}$ and $J_{cc}$ ferromagnetic interactions.

The parameters $J_{ad}, J_{cd}, J_{ac}, J_{aa}, J_{dd}$ and $J_{cc}$ could be related to the Heisenberg theory, which assumes localized atomic moments coupled through exchange integrals that depend on the overlap of nonorthogonal, atomic orbitals of neighboring atoms. In the present work, the Hamiltonian parameters $H_z$, strength of an external magnetic field and $D_i^{a,d,c}$, the crystal field, were fixed at zero. The FORTRAN code allows for including terms to take into account the noncollinear configurations. The data on YIG and GdIG could be fitted, assuming collinear spin arrangement, but in the case of other rare-earth garnets, the saturation magnetization calculated at 0 K from the Néel model, e.g. is different from that observed experimentally. This discrepancy has been attributed by Dionne[22] to canting within the "c" sublattice, which is assumed to arise from the strong anisotropy field of $R^{3+}$ ions, in comparison to the exchange field on the "c" sublattice. In these cases, it is possible to take into account the canting by D parameter. In order to avoid the overparametrization event, it was necessary to take into account previous results[5,8,16–20,25] and also to consider $J_{cc} = 0$. For the $Y_3Fe_5O_{12}$- case, $J_{ad}$, $J_{aa}$ and $J_{dd}$ remain to be determined from comparison with experimental data.[14] Since amongst the rare-earth iron garnets, $T_c$ is approximately constant, it can be assumed that the transition-ion-transition–ion interaction, $J_{ad}$, is the dominant interaction and if it is obtained from the $Y_3Fe_5O_{12}$- case, it remains constant for $Gd_3Fe_5O_{12}$ and for all Rare Earth Garnets (RE), e.g. $Ln_3Fe_5O_{12}$. For each Monte Carlo Step (MCS), one site of the lattice is picked at random and the spin state is changed. If this change results in

Table 2. Values of $|J_{ad}|$ in $cm^{-1}$ correlated with values of parameters $P_1$ (rows) and $P_2$ (columns) (was considered $T_C = 560\,K$).

| $P_2$ | $P_1$ | | | | | | |
|---|---|---|---|---|---|---|---|
| | 0.00 | 0.18 | 0.35 | 0.43 | 0.51 | 0.57 | 0.63 |
| 0.00 | 37.9 | 31.8 | 27.7 | 26.1 | 24.6 | 23.7 | 22.8 |
| 0.21 | 34.5 | 29.4 | 25.8 | 24.4 | 23.1 | 22.3 | 21.5 |
| 0.25 | 33.9 | 29.0 | 25.5 | 24.1 | 22.9 | 22.0 | 21.2 |
| 0.29 | 33.3 | 28.5 | 25.1 | 23.8 | 22.6 | 21.8 | 21.0 |
| 0.33 | 32.8 | 28.1 | 24.8 | 23.5 | 22.4 | 21.5 | 20.8 |
| 0.35 | 32.5 | 27.9 | 24.7 | 23.4 | 22.2 | 21.4 | 20.7 |
| 0.39 | 32.0 | 27.6 | 24.4 | 23.1 | 22.0 | 21.2 | 20.5 |
| 0.45 | 31.2 | 27.0 | 23.9 | 22.7 | 21.6 | 20.9 | 20.2 |
| 0.49 | 30.8 | 26.6 | 23.7 | 22.5 | 21.4 | 20.7 | 20.0 |

a lower energy, $E_i$, the change is accepted automatically; otherwise, the change is accepted with the probability[28]

$$p = e^{-\Delta E/kT} \tag{5}$$

where $\Delta E$ is the energy difference between the new and the old spin states. Configurations were generated by randomly sweeping through the lattice and flipping the spins one at a time, according to the heat-bath algorithm (i.e. to do one sweep means to visit randomly all system spins, or more precisely, to at least visit every spin once). The parameters $J_{ad}$, $J_{aa}$ or $J_{dd}$ are substituted by the following reduced parameters,

$$P_0 \equiv \frac{kT}{|J_{ad}|}, \quad P_1 \equiv \frac{J_{aa}}{|J_{ad}|}, \quad P_2 \equiv \frac{J_{dd}}{|J_{ad}|}. \tag{6}$$

We mainly present the results of 63 runs for a sample with 27 FCEC, meaning that $P_1$ and $P_2$ are fixed for each run at one of the values presented in Table 2; and for each of the 63 runs, $P_0$ is varied by Eq. (1) which gives "the cooling rate".

The critical temperatures, $T_c$ or $(P_0)_{crit.} \equiv \frac{kT_c}{|Jab|}$, were calculated by locating the inflexion point in $M_S$ versus T curve (Fig. 1). There are two regions in the left and right neighboring of $T_c$, where the critical exponents[33] $\beta$, $\gamma$ and $\alpha$ are defined by equations:

$$M(T) \sim (T_{C,N} - T)^{\beta} \quad \text{for } T \leq T_{C,N}, \quad \text{with } \beta_{\text{exp}} \in [0.33, 0.37] \tag{7}$$

$$\chi(T) \sim (T - T_{C,N})^{-\gamma} \quad \text{for } T \geq T_{C,N}, \quad \text{with } \gamma_{\text{exp}} \in [1.3, 1.4] \tag{8}$$

and

$$c(T) \sim (T - T_{CN})^{-\alpha} \quad \text{for } T \geq T_{CN}, \quad \text{with } \alpha_{\text{exp}} \leq 0.1 \tag{9}$$

for zero intensity of external magnetic field ($B_0 = 0$). Our "MCIsing" code calculates the Internal Magnetic Interaction Energy, the Specific Magnetic Heat, the Resultant and Sublattice Magnetizations, and the associated susceptibilities, with equations which are given elsewhere.[31] Figure 1 shows that Eqs. (7)–(9) display this kind of behavior in our results.

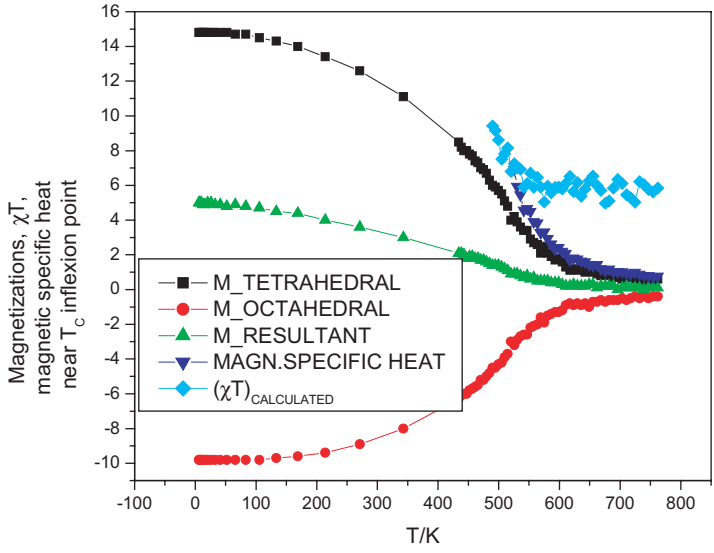


Fig. 1. Critical temperature as inflexion point in sublattices and resultant magnetizations versus temperature reduced parameter.

## 3. Results

As $J_{aa}$ and $J_{dd}$ increase, there is a monotonic increase in $T_{CN}$, reflecting the increasing of the total magnetic system energy. Variation of $(P_0)_{\text{crit.}} \equiv \frac{kT_c}{|J_{ad}|}$ with $P_1 = \frac{J_{aa}}{|J_{ad}|}$ and $P_2 = \frac{J_{dd}}{|J_{ad}|}$ is shown in Figs. 2 and 3. These results are confirmed for magnetite[3] and for layered, bimetallic ferrimagnets[32] that showed both compensate and noncompensate behavior at low temperatures.

Plane surface equation is

$$kT_C = 4.87J_{DD} + 10.86J_{AA} + 10.27|J_{AD}|. \tag{10}$$

Below the Néel (Curie) temperature of a collinear ferrimagnet is a spontaneous magnetization, just as in the ferromagnets. However, in this case, the magnetization is the vector sum of the magnetizations of the two antiparallel sublattices and therefore has magnitude

$$M_{S\_RES} = |M_{S\_DD} - M_{S\_AA}|. \tag{11}$$

As sublattice magnetizations have quite different temperature dependences, the Ms vs. T curves are not restricted to a Brillouin-type shape, as in the case of ferromagnets. Since it is shown by Srivastava *et al.*[24] that $M_S$ vs. T data could be fitted with more than one set of exchange constants, by using the molecular field approximation, it is interesting to see from Figs. 4 and 5 that based on Ising model, with the Monte Carlo-Metropolis (MCM) procedure, the computed $M_S$ vs. T curves

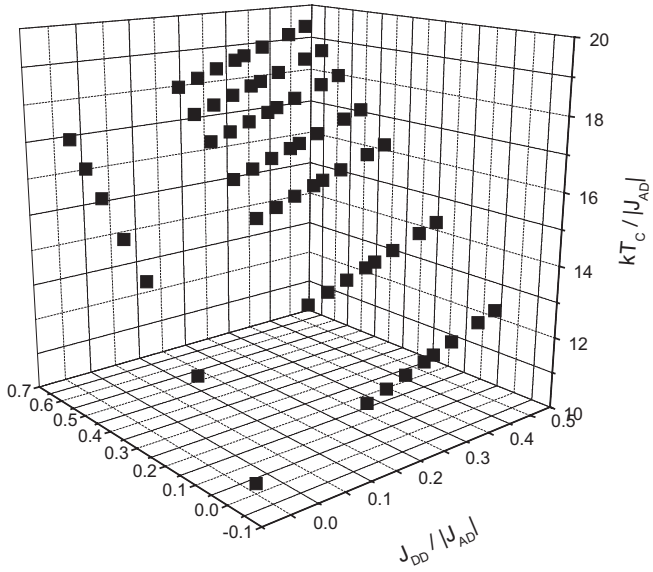


Fig. 2. $kT_C/|J_{ad}|$ versus $J_{aa}/|J_{ad}|$.

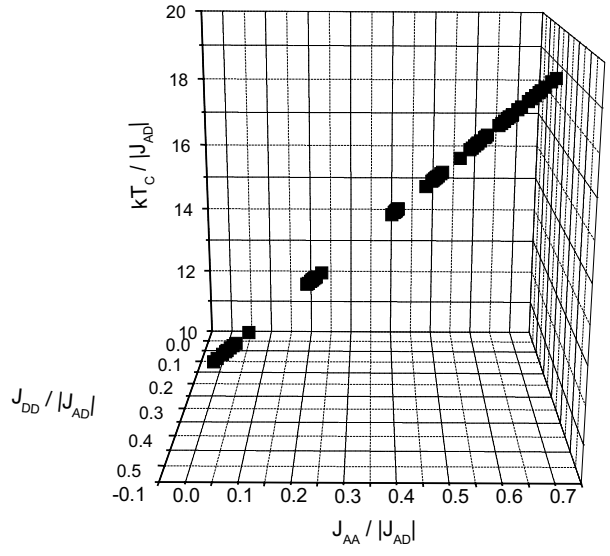


Fig. 3. $J_{dd}/|J_{ad}|$ ($P_{0\_critic}$ versus $P_1$ and $P_2$).

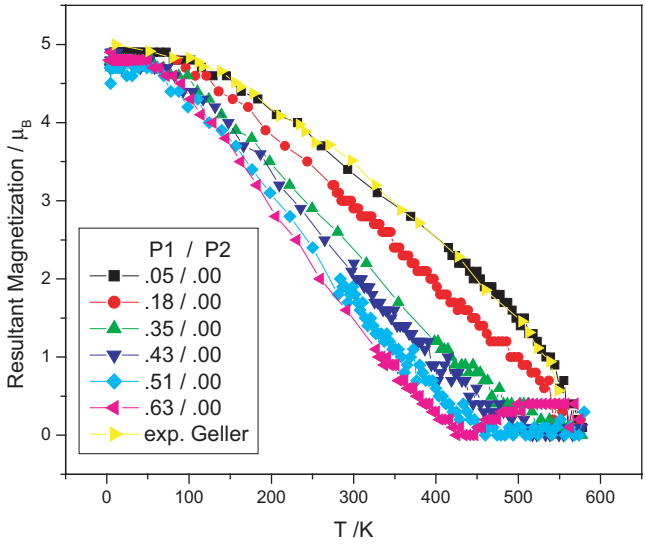


Fig. 4. Resultant spontaneous Magnetization, $M_{S\_RES}$ versus Temperature parameter, for different values of $J_{DD}/|J_{AD}|$ parameter and experimental values.[14]

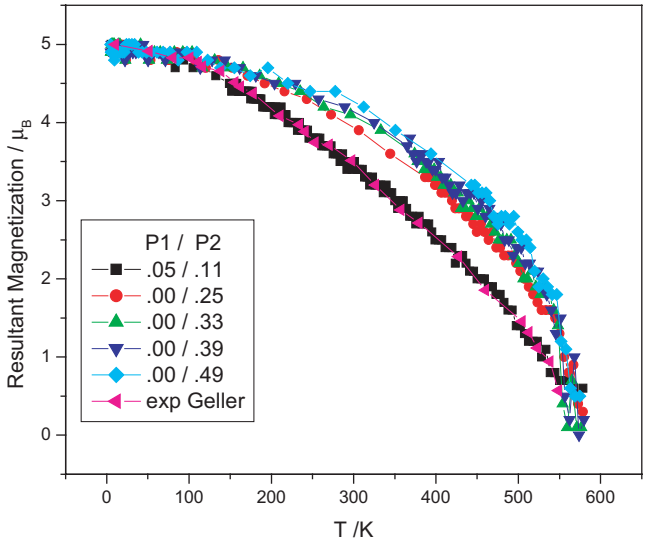


Fig. 5. Resultant spontaneous Magnetization, $M_{S\_RES}$ versus Temperature parameter, for different values of $J_{AA}/|J_{AD}|$ parameter and experimental values.[14]

for different sets of exchange constants are completely different and comparison with experimental data is possible only for

$$P_0 \equiv \frac{kT}{|J_{ad}|} = 11.2, \quad P_1 \equiv \frac{J_{aa}}{|J_{ad}|} = 0.05, \quad P_2 \equiv \frac{J_{dd}}{|J_{ad}|} = 0.11$$

or

$$J_{ad} = -34.7\,\mathrm{cm}^{-1}, \quad J_{aa} = 1.7\,\mathrm{cm}^{-1}, \quad J_{dd} = 3.9\,\mathrm{cm}^{-1},$$

values obtained by comparing calculated with experimental data.[14]

If only one sublattice is saturated or near saturation, then it is apparent that the interaction acting on the unsaturated paramagnetic ions is smaller than that acting on the saturated paramagnetic ions. Therefore, the magnetization of the unsaturated sites decreases with T faster than that of the saturated sites, so $M_{S\_RES}$ decreases if it is parallel to the unsaturated sites.

## 4. Conclusions

We have demonstrated that a comparatively simple model can reproduce ferrimagnetic behavior of garnets, particularly for $Y_3Fe_5O_{12}$ case. We have to underline that stable results capable of explaining the behavior of $Y_3Fe_5O_{12}$ garnet were obtained, considering the hypothesis above and using Ising model with Monte-Carlo procedure. It is only a matter of time for anybody to compute the parameters described, using the mentioned algorithm. We obtained $J_{ad}$, $J_{aa}$ and $J_{dd}$ parameters from measured magnetic data on YIG,[14] and considering the same hypothesis for the rest of the garnets, it will be possible to study the next "collinear case" for $Gd_3Fe_5O_{12}$, in order to obtain $J_{ac}$, and $J_{dc}$. For the next rare earth garnets, it could be necessary to use crystal field term, in order to take into account "non-collinear contributions" for rare earth garnets with important spin-orbit interaction. Since the anisotropy fields, as functions of distances and angles, are temperature-dependent, it could be possible to consider temperature dependence of parameters used in the interpretation of experimental magnetic data. It could also be possible to study the magnetic properties of 1D- or 2D-dimensional samples, devoted to understanding dimensionality effects and anisotropy.

## Acknowledgments

Nicolae Stanica would like to acknowledge the financial support from "CERES" 4–98, 5403/2004. Fanica Cimpoesu is indebted for the COE fellowship of the Japanese Society for Science.

## References

1. Eschenfelder AH, *Magnetic Buble Technology*, Springer, New York, 1981.
2. Bland JCA, Heinrich B, *Ultrathin Magnetic Structures I*, *II*, Springer, New York, 1994.

3. Stanica N, Cimpoesu F, Dobrescu G, Chihaia V, Patron L, Munteanu G, Bostan CG, *J Theor Comput Chem* **3**(2): 179–188, 2004.
4. Geller S, *Acta Cryst* **12**:944, 1959.
5. Néel L, *Ann Phys* **3**:137, 1948.
6. Menzer G, *Z Kristallogr* **69**:300, 1928.
7. Abrahams SC, Geller S, *Acta Cryst* **11**:437, 1958.
8. Bertaut EF, *J Phys IV France* **7**, 1997.
9. Prince E, *J Appl Phys* **36**:1845, 1965.
10. Hansen P, in Paoletti A (ed.), *Physics of Magnetic Garnets*, North-Holland Amsterdam, p. 56, 1978.
11. Gilleo MA, in Wohlfarth EP (ed.), *Ferromagnetic Materials*, Vol. 2, Amsterdam, North-Holland, p. 1, 1990.
12. Bonnet M, Delapalme A, Fuess H, Thomas M, *Acta Cryst* **31B**:2233, 1975.
13. Rodic D, Mitric M, Tellgren R, Rundlof H, Kremenovic A, *J Magnetism Magn Mater* **191**:137–145, 1999.
14. Geller S, Remeika JP, Williams HJ, Espinosa GP, Sherwood RC, *Phys Rev* **137A**:1034, 1965.
15. Menyuk N, Dwight K, Wold A, *J Phys Radium* **25**:528, 1964.
16. Goodenough JB, *Magnetism Chem Bond*, p. 138, 119, 199, 1963.
17. Martin DH, *Magnetism Solids* **50**:241, 1967.
18. Smit J, Wijn HPJ, *Ferrites*, John Wiley & Sons, Inc., New York, 1959.
19. Pauthenet R, *Ann Phys* (Paris) **3**:424, 1958, *Comp Rend* **230**:1842 1950; *J Phys Radium* **12**:249, 1951; *Ann Phys* **7**:710, 1952.
20. Aleonard R, *J Phys Chem Solids*, Pergamon Press, **15**:167–182, 1960.
21. Anderson EE, *Phys Rev A* **134**:1581, 1964.
22. Dionne GF, *J Appl Phys* **41**:4878, 1970; *Appl Phys* **47**:4220, 1976.
23. Riste F, Tenzer L, *Phys Chem Solids* **19**:117, 1961.
24. Srivastava CM, Srinivasan C, Nanadikar NG, *Phys Rev B* **19**:499, 1979.
25. Srivastava CM, Srinivasan C, Ayar R, *J Appl Phys* **53**(1):781, 1982.
26. Herpin A, *Théorie du magnétisme*, INSTN Saclay, 1968.
27. Onsager L, *Phys Rev* **65**:117, 1942.
28. Metropolis N, RosenBluth AW, RosenBluth MN, Teller AH, Teller E, *J Chem Phys* **21**:1087, 1953.
29. Boullant E, Cano J, Journaux Y, Decurtins S, Gross M, Pilkington M, *Inorg Chem* **40**:3900–3904, 2001.
30. Binder K, Herman DW, *Monte Carlo Simulations in Statistical Physics. An introduction*, 3rd ed., Springer, Berlin, 1997.
31. Stanica N, Munteanu G, Carp O, Patron L, Bostan CG, *Rev Roum Chim* **47** (10–11):1217, 2002.
32. Carling SG, Day P, *Polyhedron* **20**:1525–1528, 2001.
33. Ashcroft, Mermin, Solid State Physics, Thomson Learning.